Icarus 217 (2012) 839–844

Contents lists available at ScienceDirect

Icarus

journal homepage: www.elsevier.com/locate/icarus

# Upper limits for $H_2SO_4$ in the mesosphere of Venus

Brad J. Sandor [a,*], R. Todd Clancy [a], Gerald Moriarty-Schieven [b]

[a] Space Science Institute, 4750 Walnut Street, Suite 205, Boulder, CO 80301, USA
[b] National Research Council of Canada, Joint Astronomy Centre, 660 North Aohoku Place, Hilo, HI 96720, USA

ARTICLE INFO

*Article history:*
Available online 23 April 2011

*Keywords:*
Venus, Atmosphere
Photochemistry
Atmospheres, Chemistry
Atmospheres, Composition
Abundances, Atmospheres

ABSTRACT

Rapid temporal variability of $SO_2$ and SO in the Venus 85–100 km mesosphere (Sandor, B.J., Clancy, R.T., Moriarty-Schieven G.H. [2007]. Bull. Am. Astron. Soc. 39, 503; Sandor, B.J., Clancy, R.T., Moriarty-Schieven, G.H., Mills, F.P. [2010]. Icarus 208, 49–60) requires in situ sources and sinks for these molecules. While many loss mechanisms are recognized, no process for in situ production is known. Observational investigations to find, or constrain other potential sulfur reservoirs offer one method toward understanding the applicable photochemistry. Here, we report upper limits for gas-phase $H_2SO_4$ (sulfuric acid) abundances in Venus' 85–100 km upper mesosphere, derived from 16 ground-based sub-mm spectroscopic observations in the period 2004–2008. Unlike the ubiquitous sulfuric acid solid/liquid aerosol, the gas phase would be photochemically active, potentially both source and sink for SO and $SO_2$. $H_2SO_4$ is retrieved from sub-mm lines located in the same bandpass as the $SO_2$ and SO lines described by Sandor et al. (Sandor, B.J., Clancy, R.T., Moriarty-Schieven, G.H., Mills, F.P. [2010]. Icarus 208, 49–60). $H_2SO_4$ upper limits reported here are thus simultaneous and spatially coincident with measurements of $SO_2$ and SO, providing for analysis of the three sulfur species collectively. The average $H_2SO_4$ abundance over 16 observations is $1 \pm 2$ ppb (i.e. <3 ppb). Upper limits for individual observations range from 3 to 44 ppb, where quality of the observing weather is the dominant constraint on measurement precision. The sum of $H_2SO_4$, $SO_2$ and SO varies widely. In one comparison, the sum $[H_2SO_4 + SO_2 + SO]$ measured on one date differs by 10-$\sigma$ from the sum measured 2 months later. We conclude that upper mesospheric sulfur atoms are not conserved among the three molecules, that $H_2SO_4$ is not a significant sulfur reservoir for balancing the observed variations of $[SO_2 + SO]$, and is not relevant to the (still unknown) photochemistry responsible for observed behavior of $SO_2$ and SO. Having ruled out $H_2SO_4$, we infer that elemental sulfur is the most probable candidate for the needed third reservoir.



## 1. Introduction

Current chemical models of the Venus atmosphere (e.g. Yung and DeMore, 1982; Mills et al., 2007; Mills and Allen, 2007) include upward vertical transport from below the clouds as the only $SO_2$ supply mechanism to the mesosphere. Loss of mesospheric $SO_2$ proceeds via formation of $H_2SO_4$ aerosol, as either solid $H_2SO_4$, or as solid or liquid in aqueous solution. Aerosol sedimentation to lower altitudes completes the mesospheric sulfur cycle as understood through modeling. Existence of an in situ loss, but not production mechanism for mesospheric $SO_2$ requires that its model abundance can only decrease with altitude. Contrary to model expectations, observations demonstrate that $SO_2$ abundance increases with altitude (Sandor et al., 2008, 2010), such that an in situ source is required at 85–100 km altitude. While altitude dependence is time-invariant, the abundance of $SO_2$ at 85–100 km exhibits temporal variation on timescales as short as a week, requiring that the in situ source must be similarly time-variable. Sandor et al. (2007, 2010) show that SO also varies on this timescale, as do the ratio ($[SO_2]/[SO]$) and sum ($[SO_2] + [SO]$) of the two molecular abundances. Total $SO_x$ (defined as the sum $[SO_2] + [SO]$) varies from less than 3 ppb to $78 \pm 9$ ppb, such that sulfur atoms are not conserved between the two molecules. The Sandor et al. (2010) SO and $SO_2$ abundances have correlation coefficient 0.037, hence abundance variation of one molecule is not explained by chemical conversion to the other. Time variation of $SO_x$, and absence of correlation between SO, $SO_2$ abundances independently demonstrate that SO and $SO_2$ are not the only photochemically active sulfur species in Venus' upper mesosphere. Conservation of atoms requires there must be at least one additional sulfur reservoir which can act as both source and sink for SO and $SO_2$ (collectively, $SO_x$). Determining the identity of a third such sulfur-bearing molecule in the Venus upper mesosphere is prerequisite to understanding chemistry of the 85–100 km atmosphere. An observational search for other sulfur molecules is thus critical to understanding Venus.

* Corresponding author.
*E-mail address:* sandor@spacescience.org (B.J. Sandor).

0019-1035/$ - see front matter © 2011 Elsevier Inc. All rights reserved.
doi:10.1016/j.icarus.2011.03.032

The two best candidates as third sulfur reservoirs are gas-phase sulfuric acid ($H_2SO_4$) and molecular sulfur ($S_n$, where $n = 1–8$). There is no compelling theoretical basis for existence of any third sulfur reservoir. Indeed, conventional theory (e.g. Yung and DeMore, 1982) predicts there are none. However, observational evidence requires a third reservoir, hence motivates a search for sulfur molecules that conventional theory predicts are absent. The suggestion of $H_2SO_4$ and $S_n$ as candidate molecules is based on their essential role in chemistry at and below cloud level, where they are ubiquitous over significant altitude ranges. Also, sulfuric acid is known to be present in aerosol form throughout the mesosphere, where it is theoretically understood to be a sink (but not obviously a source) for $SO_x$. The conventional argument against sulfuric acid is that its very low vapor pressure at Venus mesospheric temperatures requires the gas phase abundance to be minimal (detailed below), despite that its abundance in photochemically-inactive solid phase and aqueous solution is significant. The theoretical argument against $S_n$ is that it should be photolyzed to S atoms rapidly in the dayside upper mesosphere. Hence, $S_n$ might be theoretically plausible if observed $SO_x$ abundance variations were purely diurnal, but they are not. $SO_x$ is strongly variable during both day and night, and there is no evidence that time-averaged total $SO_x$ on the nightside differs from that on the dayside (Sandor et al., 2010).

$H_2SO_4$ saturation vapor pressure increases with temperature and decreases in the presence of liquid water. Sub-mm observations of SO, $SO_2$ (Sandor et al., 2010) are made at horizontal resolution 4000–12,000 km, such that measured abundances reflect mean conditions over regions of that size, and at 85–100 km altitude. Temperature measurements at the same spatial scale (Clancy et al., 2011) are in the range 170–200 K. Warmest reported temperatures, based upon Venus Express observations (Bertaux et al., 2007) at much smaller spatial scales, indicate values 200–230 K above 90 km. Laboratory data (Roedel, 1979; Ayers et al., 1980) find the saturation vapor pressure of $H_2SO_4$ to be $10^{-16}$–$10^{-10}$ hPa (mbar) for temperatures 170–230 K (respectively), when water is absent. Pressure at 85 km is 10 hPa, such that at 230 K the saturated $H_2SO_4$ abundance for this temperature range is 10 parts per trillion (0.010 ppb). At 100 km the pressure is 0.02 hPa, allowing maximum saturated abundance of 5 ppb at 230 K. In the presence of water, $H_2SO_4$ readily dissolves, and saturated vapor pressure decreases with decreasing concentration of the acid. When aqueous sulfuric acid is present at 75% solution, saturation vapor pressure is smaller by three orders of magnitude (Ayers et al., 1980; Marti et al., 1997) than when water is absent.

Zhang et al. (2010) present a novel theoretical approach in which the Sandor et al. (2010) $SO_2$ can be understood in terms of large abundances of $H_2SO_4$, 1 ppb at 92 km, 100 ppb at 95 km, and 3000 ppb at 98 km altitude. Limitations of $H_2SO_4$'s low vapor pressure are addressed by first assuming the maximum temperatures measured with the SPICAV instrument on board the Venus Express (VE) spacecraft (Bertaux et al., 2007), which are much warmer than temperatures measured with other observing platforms (e.g. ground-based microwave (Clancy and Muhleman, 1991; Lellouch et al., 1994; Clancy et al., 2003, 2007, 2008, 2011); Pioneer Venus (PV) descent probes (Seiff et al., 1980); PV Orbiting IR radiometer (Schoeld and Taylor, 1983). Second, Zhang et al. (2010) assume large supersaturation factors for the $H_2SO_4$ vapor over solid phase, and/or $H_2SO_4$ photolysis cross-sections much larger than currently accepted values (Lane and Kjaergaard, 2008). The Zhang et al. (2010) model can produce the required $H_2SO_4$ either with laboratory measured cross-sections combined with 1100% supersaturation, or with cross-sections increased by a factor of 30 combined with no supersaturation. The Zhang et al. (2010) conditions are extreme, and may reflect over-simplifications of the chemistry. For example, Zhang et al. (2010) point to $H_2SO_4$ hydrates as potentially important, yet such hydrates are not included in their model. In any case, Zhang et al. (2010) suggest that large $H_2SO_4$ abundances may solve the upper mesospheric sulfur chemistry problem.

This study is an observational search for gas-phase $H_2SO_4$ in the Venus upper mesosphere. Ground-based sub-mm spectroscopic observations of Venus for $H_2SO_4$ were conducted in the period 2004–2008. Observations and their analysis are described in Section 2. Results are presented in Table 1, and discussed in Section 3. Table 1 includes measured values of SO and $SO_2$, providing context for this $H_2SO_4$ study in terms mesospheric sulfur abundances. Fig. 1 illustrates that SO and $SO_2$ abundances are uncorrelated. This is

**Table 1**
Measured abundances of $H_2SO_4$, $SO_2$, and SO in the Venus upper mesosphere.

| Geometry | | | VMR (ppbv) | | | | | | |
|---|---|---|---|---|---|---|---|---|---|
| Date | Phase | $D$ | $H_2SO_4$ | | | $SO_x$ | | | $SO_2 + SO + H_2SO_4$ |
| | | | Value | 1-$\sigma$ limit | 2-$\sigma$ limit | $SO_2$ | SO | $SO_2 + SO$ | |
| 12 June 2004 | 0.005 | 57″ | −3 ± 10 | 7 | 17 | 25 ± 9 | 0 ± 2 | 25 ± 9 | 25(+12; −9) |
| 14–15 January 2006 | 0.005 | 63″ | 1 ± 11 | 12 | 23 | 11 ± 3 | 1 ± 1 | 12 ± 3 | 13(+11; −3) |
| 14 January 2007 | 0.948 | 11″ | −4 ± 26 | 22 | 48 | 11 ± 6 | 3 ± 2 | 14 ± 6 | 14(+23; −6) |
| 20–21 January 2007 | 0.940 | 11″ | 0 ± 17 | 17 | 34 | 13 ± 4 | 9 ± 2 | 22 ± 4 | 22(+18; −4) |
| 21 April 2007 | 0.721 | 15″ | 2 ± 9 | 11 | 20 | 35 ± 10 | 13 ± 2 | 48 ± 10 | 50(+14; −11) |
| 22 April 2007 | 0.718 | 15″ | −2 ± 5 | 3 | 8 | 30 ± 5 | 10 ± 1 | 40 ± 5 | 40(+6; −5) |
| 29 April 2007 | 0.691 | 16″ | 2 ± 7 | 9 | 16 | 27 ± 4 | 15 ± 1 | 42 ± 4 | 44(+8; −5) |
| 2 June 2007 day | 0.536 | 22″ | 2 ± 13 | 15 | 28 | 4 ± 2 | 2.3 ± 0.5 | 6 ± 2 | 8(+13; −3) |
| 9 June 2007 night | 0.498 | 24″ | 0 ± 6 | 6 | 12 | 0 ± 2 | 1.0 ± 0.3 | 1.0(+2.0; −0.3) | 1(+6; −0.3) |
| 9 June 2007 day | 0.498 | 24″ | 2 ± 8 | 10 | 18 | 0 ± 3 | 2.1 ± 0.5 | 2.1(+3.0; −0.5) | 4(+9; −4) |
| 11 August 2007W | 0.000 | 56″ | 1 ± 7 | 8 | 15 | 76 ± 9 | 1.7 ± 1.3 | 78 ± 9 | 79(+11; −9) |
| 11 August 2007N | 0.000 | 56″ | 1 ± 5 | 6 | 11 | 50 ± 11 | 1.0 + 0.7 | 51 ± 11 | 52(+12; −11) |
| 11 August 2007S | 0.000 | 56″ | 2 ± 6 | 8 | 14 | 67 ± 6 | 0.0 ± 0.7 | 67 ± 6 | 69(+9; −6) |
| 23 March 2008 | 0.940 | 11″ | 6 ± 29 | 35 | 64 | 7 ± 4 | 9 ± 3 | 16 ± 5 | 22(+29; −8) |
| 8 August 2008 | 0.958 | 10″ | −2 ± 36 | 34 | 70 | 26 ± 13 | 15 ± 3 | 41 ± 13 | 41(+37; −13) |
| 17 August 2008 | 0.945 | 10″ | 6 ± 38 | 44 | 82 | 38 ± 16 | 31 ± 4 | 69 ± 16 | 75(+41; −18) |
| Mean | | | 1 ± 2 | 3 | 5 | 23 ± 1 | 7.5 ± 0.2 | | |

$D$ is the angular diameter of Venus (arcsec). Measured volume mixing ratios, their 1-$\sigma$ s/n uncertainties, and volume mixing ratio upper limits have units of parts per billion (ppb). $SO_2$ and SO abundances are at altitudes of 85–100 km (Sandor et al., 2010) $H_2SO_4$ abundances and upper limits are retrieved assuming the same altitude distribution as for $SO_2$ and SO. The August 11, 2007 observations were at positions West, North, and South of disc center, all on Venus nightside. June 2007 observations were at points East and West of center, corresponding to nightside and dayside, respectively. Measurements on dates outside of June and August 2007 are of disc average values.

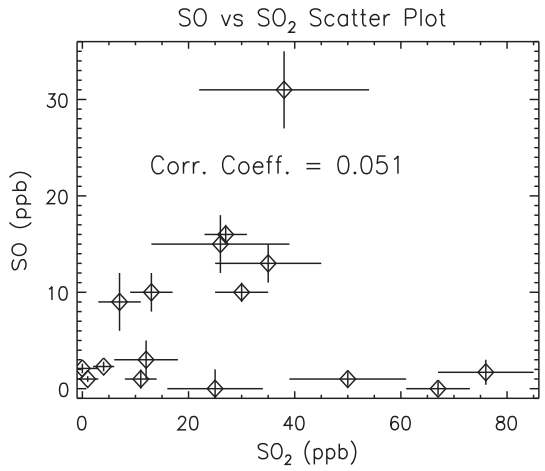


**Fig. 1.** Measured SO and $SO_2$ mixing ratios (Table 1) are presented here as a scatter plot. Abundances of the two molecules are not correlated.

one demonstration that sulfur atoms are not conserved by SO + $SO_2$, hence that a third sulfur reservoir is required. Representative spectroscopic data are presented in Figs. 2 and 3. Fig. 3 also includes synthetic, model spectra generated as part of the data analysis procedure. Measurement results are that data provide stringent upper limits, but no detections of $H_2SO_4$. Conclusions, also discussed in Section 3, include that $H_2SO_4$ cannot be the third sulfur reservoir needed to understand observed $SO_x$ temporal variations. This leaves molecular sulfur as the best candidate species for that third photochemically active sulfur molecule.

## 2. Observations and data analysis

From 2004 to the present we have conducted spectroscopic observations for $SO_2$, SO, and $H_2SO_4$ in the Venus atmosphere. Venus observations of sub-mm lines of $SO_2$ (346.65217 GHz), SO (346.52848 GHz), and $H_2SO_4$ (346.58020 GHz) are obtained with the James Clerk Maxwell Telescope (JCMT), located on Mauna Kea, Hawaii (Matthews, 2003). Our sulfur chemistry research is based upon spectra centered at 346.590 GHz, with a bandpass width of at least 250 MHz. This spectral region was chosen because it includes strong lines of $SO_2$, SO, and $H_2SO_4$, such that spectroscopic line positions of the three molecules are observed simultaneously. Relative spectroscopic strengths of the lines are $SO:SO_2:H_2SO_4$ = 9.6:2.0:1.0. Observation sensitivity (per unit mixing ratio) to $H_2SO_4$ is half the sensitivity to $SO_2$, and 10% the sensitivity to SO. The first detections of $SO_2$ and SO were obtained in 2004 and 2007, respectively. Routine inspection of the data by eye has not yielded any sulfuric acid detection. Rigorous $H_2SO_4$ retrievals are presented here for the first time, based upon the same spectra used by Sandor et al. (2010) to retrieve $SO_x$ abundances. $H_2SO_4$ is below detection thresholds of all analyzed spectra, such that an upper limit is determined from each data spectrum. Methods of observation and data analysis, as previously described by Sandor et al. (2010), are only summarized in the present work. Issues specific to $H_2SO_4$ are treated in detail.

Altitude resolution is determined from radiative transfer analysis of the pressure-broadened sub-mm absorption line. At the lowest pressures (highest altitudes), absorption occurs only at line center. Observations described in the present work are sensitive to 70–100 km altitudes in the Venus atmosphere, with maximum sensitivity (per unit mixing ratio) at 80–85 km. The 70 km lower altitude limit corresponds to a pressure-broadened linewidth that exceeds a practical bandwidth of measurement. The 100 km upper altitude limit is determined by vanishing signal at low atmospheric density, and applies to species with abundances roughly constant, or linearly increasing with altitude. Measurement sensitivity extends above 100 km for molecules that exhibit exponential increase of mixing ratio with altitude (e.g. CO (Clancy et al., 2003, 2008, 2011) or the Zhang et al. (2010) model $H_2SO_4$ abundances). Absorption of these optically thin lines is linearly

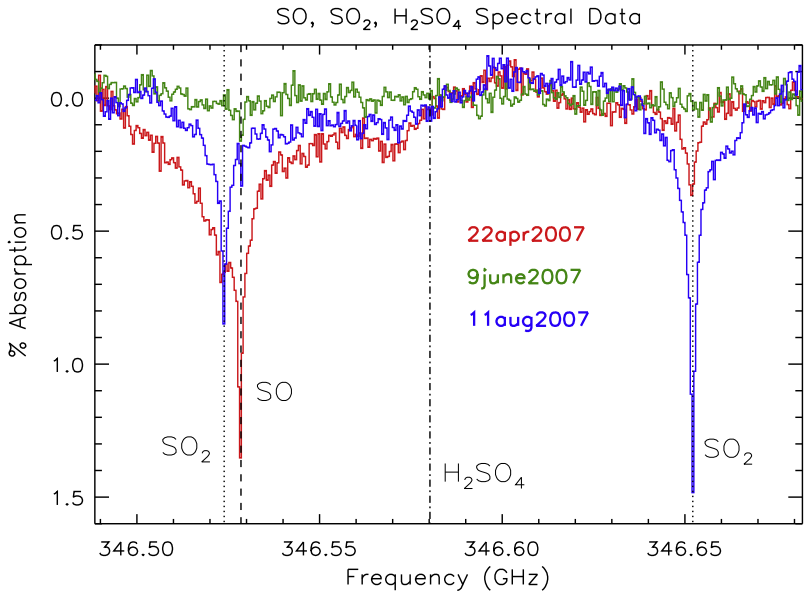


**Fig. 2.** Venus spectra from April 22 (red), June 9 (green), and August 11 (blue) 2007. Line frequencies corresponding to $SO_2$ (dotted), SO (dashed), and $H_2SO_4$ (dot–dashed) are indicated. This June 9 spectrum (green) is the average of spectra simultaneously observed at East (nightside) and West (dayside) positions on the planet. Similarly, the presented August 11 (blue) spectrum is the average of spectra simultaneously observed at West, North, and South Venus positions. Retrieved abundances for each of the two June spectra, and each of the three August spectra are listed in Table 1. Total $SO_x$ (SO + $SO_2$) was 40 ± 5 ppb on April 22, less than 4 ppb on June 9, and 65 ± 5 ppb on August 11. The April spectrum determines far more SO than $SO_2$, while the August spectrum shows much less SO than $SO_2$. The $H_2SO_4$ is undetectable for all observed $SO_x$ abundance scenarios. (For interpretation of the references to color in this figure legend, the reader is referred to the web version of this article.)

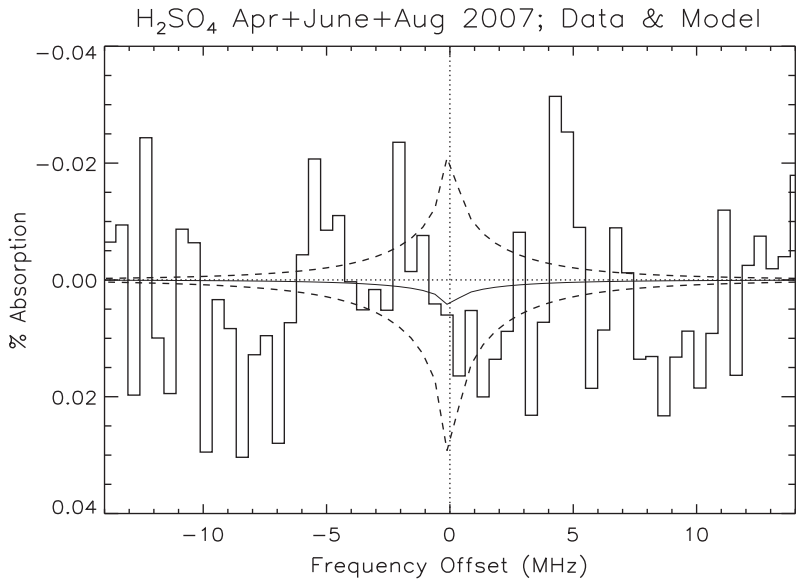


**Fig. 3.** The average of the three Fig. 2 data spectra is presented here (histogram) for the 28 MHz range centered on the $H_2SO_4$ line frequency. $H_2SO_4$ abundance retrieved from these data is 0.5 ± 3 ppb. The best-fit synthetic line, corresponding to 0.5 ppb, is shown as a solid curve. Dashed curves are synthetic spectra corresponding to −2.5 ppb, and to +3.5 ppb, the one sigma bounds about the best fit value.

proportional to the temperature contrast between the absorbing layer, and the deeper layer at which the atmosphere becomes optically thick. Measurement sensitivity to temperature errors is thus low, contributing 5% uncertainty to retrieved $H_2SO_4$ abundances.

Spectroscopic line parameters were obtained from the JPL microwave spectroscopy database (Pickett et al., 1996, 1998; Poynter and Pickett, 1985). The $H_2SO_4$ absorption derives from two spectroscopic lines, separated by 5.5 KHz. The lower frequency line, at 346.5802036 GHz, corresponds to the $N = 34 \rightarrow 33$, $K_{-1} = 24 \rightarrow 23$, $K_{+1} = 10$ transition. The higher frequency line, at 346.5802091 GHz, corresponds to the $N = 34 \rightarrow 33$, $K_{-1} = 24 \rightarrow 23$, $K_{+1} = 11$ transition. Minimum thermal width of each line at Venus atmospheric temperatures is 130 KHz, a factor of 20 greater than the 5.5 KHz separation between lines, such that the two lines are not resolved by observation. Hence, calculation of synthetic $H_2SO_4$ absorption formally models the absorption feature as the sum of two closely spaced spectroscopic lines. Observations prior to 2007 were made with spectral resolution 313 KHz. Following a hardware upgrade at the JCMT, observations from 2007 to present were made at resolutions of 30.5, 61.0, or 488 KHz.

The JCMT has a 15 m primary mirror, which at the 346.6 GHz frequency of our observations provides a gaussian shaped beam with full width half power (FWHP) beam footprint of 13″. The diameter of Venus varies between 9.6″ and 60″ at superior and inferior conjunctions, respectively. Spatial resolution at horizontal scales smaller than the sub-Earth hemisphere is possible for Venus diameter larger than 22″, corresponding to phase less than 0.57, and to Venus size exceeding the FWHP beam footprint diameter by a factor of 1.7. For Venus diameter <22″, all observations are made with the telescope pointed to the center of Venus' projected sub-Earth disc, such that measurements are hemispheric mean values. For larger diameters, 22″–60″, offsetting the telescope beam from disc center provides both spatially resolved data (by analysis of individual beam positions), and hemispheric mean determinations (by analysis of data averaged over beam positions). For this study, spatially resolved data were analyzed only from observations conducted in June and August, 2007. All other analyzed spectra correspond to hemispheric mean observations.

$H_2SO_4$ abundances were retrieved from the same spectra used by Sandor et al. (2010) to retrieve $SO_2$ and SO abundances. Therefore, the $SO_2$, SO observational procedures apply directly to the $H_2SO_4$ observations presented here, and the observational method is described here only in summary form. Details may be found in Sandor et al. (2010). Beam switching is employed, in which the telescope alternately observes Venus and a nearby sky positions away from Venus. Spectra from the sky are subtracted from those of Venus, such that background emission (primarily Earth's atmosphere) is removed from the Venus data. The $H_2SO_4$ line is seen as an absorption, as $H_2SO_4$ (or any gas) in the 70–100 km region to which the observations are sensitive is colder than the continuum blackbody radiation emitted from the warmer, lower atmosphere. Spherical geometry of the Venus atmosphere is incorporated in analysis of each observation, allowing for absorption contributions from various slant paths across the face of the disk, as well as for limb emission (Clancy and Muhleman, 1991). Data are interpreted as fractional absorption from the continuum, wherein depth of absorption is divided by the continuum signal. Calibrating spectral absorption with this method requires accurate modeling of continuum emission from the deep atmosphere, for which we compare observed signal level far from line center to observations and models of the sub-mm continuum from below ~70 km (e.g. Muhleman et al., 1973). Uncertainty in the observed continuum signal level is negligible, typically <±0.03%, such that uncertainty in the observed absorption from continuum is dominated by a 1% uncertainty in the receiver's rejection of the image sideband, translating into a 1% uncertainty in the measured $H_2SO_4$ mixing ratio. Continuum modeling includes spherical geometry of Venus convolved with the telescope beam shape, a temperature profile of the atmosphere below 70 km, and radiative transfer calculations to determine the altitude range from which our observations measure the continuum (Muhleman et al., 1973). Uncertainties in modeling the continuum emission introduce $\leqslant$10% uncertainty in the derived $H_2SO_4$ abundances. Uncertainties from observed (1%) and model ($\leqslant$10%) continuum levels add in quadrature, such that together they contribute 5–10% uncertainty to the retrieved $H_2SO_4$ abundance associated with all sources of uncertainty in the continuum level. Uncertainties associated with the continuum contribute only to systematic errors. They have no effect on precision, hence no effect variation among measurements. Uncertainties in the telescope beam size (±1″) and

pointing ($\leqslant 5''$) (Matthews, 2003) are too small to impact retrieved abundances.

The depth of microwave absorption scales linearly with the temperature contrast between the atmosphere at the altitude where continuum emission becomes optically thick, and the atmosphere where absorption from the continuum occurs. Temperature profiles used in our retrievals are specific to the Venus phase of each observation, and are based upon the diurnal profiles of Clancy et al. (2003). The source of temperature uncertainty is secular variation of temperature away from the diurnal climatology. Such variations are negligible at 85 km, and grow with altitude to perhaps ±10 K at 100 km. We conservatively estimate temperature uncertainty to be ±5 K over the 85–100 km altitude range, the effect of which is a ±7% uncertainty in retrieved $H_2SO_4$.

The pressure broadening constant for $H_2SO_4$ is unknown. We estimate the pressure broadening coefficient of $H_2SO_4$ as identical to that for $SO_2$ at 346.52388 GHz, and estimate the uncertainty in application to $H_2SO_4$ as ±30%. The corresponding uncertainty in retrieved $H_2SO_4$ is ±20%.

The largest source of uncertainty in measured abundances is contributed by noise (s/n) constraints. Spectral noise is defined as random channel-to-channel variations in brightness temperature of the observed absorption spectrum. Noise is decreased (s/n is improved) by increased observation time (such that the average of the random variations becomes small relative to the $SO_x$ absorption signal), and by excellent observing conditions (very low water abundance in the terrestrial atmosphere above the telescope).

Spectrometer baselines include artifacts, primarily low-amplitude waves manifesting as sinusoidal variations in continuum level as a function of frequency. These artifacts vary among the observations, and during each individual integration. Their sources are not quantitatively understood, such that there is no a priori basis for the observatory software to remove them from the receiver output. Most can be identified by inspection as sinusoidal wave forms, which can be fit and removed during analysis. In general, wave artifacts are not in phase with any absorption signal, and have wavelengths significantly longer than twice the width of the absorption, such that negligible uncertainty results from their removal. In the minority of cases where a wave is in phase with an absorption and has wavelength that mimics absorption width, the spectrum is discarded.

Remaining baseline irregularities contribute to retrieval uncertainties, and can be significant when the noise level is small. Our calculated s/n uncertainties include effects of both true noise (random, channel-to-channel variation of the signal level), and these baseline artifacts.

## 3. Results and conclusion

Results of $H_2SO_4$ retrievals are listed in Table 1, together with the $SO_x$ abundances retrieved from the same spectra (Sandor et al., 2010). Relative to that publication, SO retrievals for June 2004 and January 2006 are new. Spectra from January 14 and 15, 2006 are combined for improved s/n, as are the January 20 and 21, 2007 data.

A scatter plot of Table 1 $SO_x$ abundances is presented Fig. 1, illustrating there is no correlation between retrieved $SO_2$ and SO abundances. Spectra from April 22, June 9, and August 11, 2007 are shown in Fig. 2. Positions of the SO, $SO_2$, and $H_2SO_4$ spectroscopic lines, indicated in Fig. 2, are all within a 250 MHz spectrometer bandpass, such that observations of the three molecules are always simultaneous. $SO_x$ abundances in the three Fig. 1 spectra are very different. April has large SO, and much smaller $SO_2$ abundance. Conditions are reversed in August 11, when there is little SO, and much larger $SO_2$ abundance. In June, $SO_x$ abundances are small. On all three dates, and under all conditions of $SO_x$ abundance, $H_2SO_4$ is undetectable.

Synthetic spectra were generated from model $H_2SO_4$ altitude profiles. Model profiles assume zero abundance below 84 km, and nonzero constant (altitude-invariant) $H_2SO_4$ above 84 km. This altitude dependence was adopted in Sandor et al. (2010) to model $SO_x$ above 84 km. Each $H_2SO_4$ abundance is retrieved by subtracting synthetic spectra, corresponding to a range of $H_2SO_4$ abundances, thereby generating a residuals (data – synthetic) spectrum associated with each $H_2SO_4$ abundance used to generate synthetic spectra. The summed squared residuals are calculated for each difference spectrum, with residuals weighted by the strength of the synthetic absorption at each offset frequency, relative to its line center absorption. The synthetic spectrum corresponding to the smallest value of the summed squared residuals is identified as the best fit to data. The model $H_2SO_4$ abundance used to generate that spectrum is the retrieved abundance.

Uncertainty in the retrieved abundance is determined by calculating synthetic spectra corresponding to the best fit abundance ±$X$, where $X$ is an estimated abundance uncertainty. Those two spectra (plus and minus) form an envelope about the best fit spectrum. The envelope that contains 68% of the difference between the data and best fit spectra is by definition the 1-$\sigma$ envelope. The value of $X$ that generates this envelope is the 1-$\sigma$ uncertainty in the retrieved $H_2SO_4$ abundance.

Fig. 3 presents the average of the three Fig. 1 spectra (histogram), for the 28 MHz range centered on the $H_2SO_4$ line frequency. The best-fit synthetic spectrum is represented by the solid curve. Dashed curves correspond to the 1-sigma envelope about the best fit. The $H_2SO_4$ abundance retrieved from this spectrum is 0.5 ± 3 ppb. Averaging abundances retrieved from the individual spectra (Table 1), and combining their uncertainties yields 0.2 ± 2.6 ppb, consistent with retrieval from the averaged spectra. Given the retrieval error bars, each of these measurements represents an upper limit rather than a detection for $H_2SO_4$.

The fourth column of Table 1 lists the retrieved $H_2SO_4$ abundance and 1-$\sigma$ uncertainty for each observation. Again, all measured values are within 1-$\sigma$ of zero, such that each measurement represents an upper limit. Four of the fifteen retrieved abundances are negative. While not intuitive, negative values are a necessary consequence for any system that measures values that are less than or comparable to the measurement uncertainty. The physical interpretation of (e.g.) −3 ± 10 ppbv is zero abundance, with one- and two-$\sigma$ upper limits of 7 and 17 ppbv, respectively.

All 16 measured abundances differ from zero by less than 1-$\sigma$, in conflict with the basic property of gaussian distributions that 32% of measured values should differ from the true value by more than 1-$\sigma$, i.e. if the true $H_2SO_4$ abundance is undetectable with a measurement system, 32% of the measurements should be (positive or negative) values that differ from zero by more than 1-$\sigma$. It follows that Table 1 $H_2SO_4$ abundance uncertainties are overestimated.

The average of the 16 measured $H_2SO_4$ abundances (Table 1) is 1 ± 2 ppbv, where the 2 ppb uncertainty is calculated from uncertainties of the individual measurements. It follows immediately that the $H_2SO_4$ 1- and 2-$\sigma$ upper limits for the average of our observations are 3 ppb and 5 ppb, respectively. If $H_2SO_4$ abundance in the upper mesosphere is time-invariant, then 3 and 5 ppb can be interpreted as the 1- and 2-$\sigma$ upper limits of that invariant abundance. If $H_2SO_4$ abundance is time variable, then there may isolated times when its mixing ratio exceeds the mean 1 ppb by many sigma. No such isolated event has been observed to date.

The fifth and sixth columns of Table 1 lists the 1- and 2-$\sigma$ $H_2SO_4$ upper limits for each observation date. Mean values of the upper limits, 3 and 5 ppb, are based upon the mean measured abundance of 1 ± 2 ppbv.

Columns 7, 8, and 9 of Table 1 list the $SO_x$ abundances from Sandor et al. (2010). Column 9, total $SO_x$, illustrates the conclusion from that study that sulfur atoms are not conserved among SO and $SO_2$. Column 10 lists total abundances of all three gases, SO, $SO_2$, and $H_2SO_4$, addressing whether sulfur atoms can be conserved with inclusion of $H_2SO_4$. It is calculated as the sum of the three retrieved abundances, with negative abundances treated as zero. Uncertainties of the three molecule sum are calculated with the constraint that we know molecular abundances cannot be negative.

The 5-$\sigma$ *upper* bound for the three molecule sum on the June 9, 2007 nightside hemisphere is 31 ppb, while the 5-$\sigma$ *lower* bound for this sum at the August 11, 2007 South position (also nightside) is 39 ppb, i.e. the 5-$\sigma$ bounds of these two measurements, separated in time by 2 months, do not overlap. We conclude that sulfur atoms in the Venus upper mesosphere are not conserved among SO, $SO_2$, and $H_2SO_4$.

This study observationally determines $H_2SO_4$ 1- and 2-$\sigma$ upper bounds of 3 and 5 ppb, respectively, orders of magnitude smaller than $H_2SO_4$ abundances required by the Zhang et al. (2010) model to generate $SO_2$ abundances observed by Sandor et al. (2010). It follows that that photochemically active $H_2SO_4$ plays no role in sulfur chemistry of the Venus upper mesosphere. We suggest $S_n$ as the most probable third sulfur reservoir, required by observed $SO_2$, SO abundances for conservation of sulfur atoms.

## Acknowledgments

We are indebted to the excellent telescope system specialists of the James Clerk Maxwell Telescope (JCMT) on Mauna Kea – Jim Hoge, Jonathan Kemp, and Ben Warrington – as well as the JCMT staff at the Joint Astronomy Centre in Hilo, Hawaii. The JCMT is operated by the Joint Astronomy Centre on behalf of the Science and Technology Facilities Council of the United Kingdom, the Netherlands Organization for Scientific Research, and the National Research Council of Canada. We thank Y. Yung and C. Parkinson for scientific discussions of their $H_2SO_4$ modeling work. Investigators Sandor and Clancy were supported by the National Science Foundation under Grant No. AST-0607493, and by NASA under Grant No. NNX10AB33G, toward completion of this research. Any opinions, findings, and conclusions or recommendations expressed in this material are those of the author(s) and do not necessarily reflect the views of the National Science Foundation, or the views of NASA.

## References

Ayers, G.P., Gillet, R.W., Gras, J.L., 1980. On the vapor pressure of sulfuric acid. Geophys. Res. Lett. 7, 433–436.

Bertaux, J.L. et al., 2007. A warm layer in Venus cryosphere and high-altitude measurements of HF, HCl, $H_2O$ and HDO. Nature 450, 646–649.

Clancy, R.T., Muhleman, D.O., 1991. Long-term (1979–1990) changes in the thermal, dynamical, and compositional structure of the Venus mesosphere as inferred from microwave spectral observations of $^{12}CO$, $^{13}CO$, and $C^{18}O$. Icarus 89, 129–146.

Clancy, R.T., Sandor, B.J., Moriarty-Schieven, G.H., 2003. Observational definition of the Venus mesopause: Vertical structure, diurnal variation, and temporal instability. Icarus 161, 1–16.

Clancy, R.T., Sandor, B.J., Moriarty-Schieven, G.H., 2007. Dynamics of the Venus upper atmosphere: Global-temporal distribution of winds, temperature, and CO at the Venus mesopause. Bull. Am. Astron. Soc. 39, 539–540.

Clancy, R.T., Sandor, B.J., Moriarty-Schieven, G.H., 2008. Venus upper atmospheric CO, temperature, and winds across the afternoon/evening terminator from June 2007 JCMT sub-millimeter line observations. Planet. Space Sci. 56, 1344–1354.

Clancy, R.T., Sandor, B.J., Moriarty-Schieven, G.H., 2011. Thermal structure and CO distribution for the Venus mesosphere/lower thermosphere: 2000–2009 inferior conjunction sub-millimeter CO absorption line observations. Icarus, submitted for publication.

Lane, J.R., Kjaergaard, H.G., 2008. Calculated electronic transitions in sulfuric acid and implications for its photodissociation in the atmosphere. J. Phys. Chem. A 112, 4958–4964.

Lellouch, E., Goldstein, J.J., Rosenqvist, J., Bougher, S.W., Paubert, G., 1994. Global circulation, thermal structure, and carbon monoxide distribution in Venus mesosphere in 1991. Icarus 110, 315–339.

Matthews, H.E., 2003. The James Clerk Maxwell Telescope: A Guide for the Prospective User. Joint Astronomy Centre, Hilo, Hawaii, February 20, 2003. <www.jach.hawaii.edu>.

Marti, J.J., Jefferson, A., Cai, X.P., Richert, C., McMurry, P.H., Eisele, F., 1997. $H_2SO_4$ vapor pressure of sulfuric acid and ammonium sulfate solutions. J. Geophys. Res. 102, 3725–3735.

Mills, F.P., Allen, M., 2007. A review of selected issues concerning the chemistry in Venus' middle atmosphere. Planet. Space Sci. 55, 1729–1740.

Mills, F.P., Esposito, L.W., Yung, Y.L., 2007. Atmospheric composition, chemistry, and clouds. In: Esposito, L.W., Stofan, E.R., Cravens, T.E. (Eds.), Exploring Venus as a Terrestrial Planet, Geophysical Monograph Series, vol. 176. American Geophysical Union, pp. 73–100.

Muhleman, D.O., Berge, G.L., Orton, G.S., 1973. The brightness temperature of Venus and the absolute flux-density scale at 608 MHz. Astrophys. J. 183, 1081–1085.

Pickett, H.M., Poynter, R.L., Cohen, E.A., Delitsky, M.L., Pearson, J.C., Muller, H.S.P., 1996. Submillimeter, millimeter, and microwave spectral line catalog, JPL Publ. 80-23, Jet Propul. Lab., Pasadena, CA.

Pickett, H.M., Poynter, R.L., Cohen, E.A., Delitsky, M.L., Pearson, J.C., Muller, H.S.P., 1998. Submillimeter, millimeter, and microwave spectral line catalog. J. Quant. Spectrosc. Radiat. Transf. 60, 883–890.

Poynter, R.L., Pickett, H.M., 1985. Submillimeter, millimeter, and microwave spectral line catalog. Appl. Opt. 24, 2235–2240.

Roedel, W., 1979. Measurement of sulfuric acid saturation vapor pressure; Implications for aerosol formation by heteromolecular nucleation. J. Aerosol Sci. 10, 375–386.

Sandor, B.J., Clancy, R.T., Moriarty-Schieven, G.H., 2007. SO and $SO_2$ in the Venus mesosphere: Observations of extreme and rapid variation. Bull. Am. Astron. Soc. 39, 503 (Abstract No. 45.08).

Sandor, B.J., Clancy, R.T., Moriarty-Schieven, G.H., Mills, F.P., 2008. Diurnal and altitude behavior of SO and $SO_2$ in the Venus mesosphere. Bull. Am. Astron. Soc. 40, 514 (Abstract No. 62.02).

Sandor, B.J., Clancy, R.T., Moriarty-Schieven, G.H., Mills, F.P., 2010. Sulfur chemistry in the Venus mesosphere from $SO_2$ and SO microwave spectra. Icarus 208, 49–60.

Schoeld, J.T., Taylor, R.W., 1983. Measurements of the mean, solar-fixed temperature and cloud structure of the middle atmosphere of Venus. Q. J. R. Meteorol. Soc. 109, 57–80.

Seiff, A., Kirk, D.B., Young, R.E., Blanchard, R.C., Findlay, J.T., Kelly, G.M., Sommer, S.C., 1980. Measurements of thermal structure and thermal contrasts in the atmosphere of Venus and related dynamical observations: Results from the four Pioneer Venus probes. J. Geophys. Res. 85, 7903–7933.

Yung, Y.L., DeMore, W.B., 1982. Photochemistry of the atmosphere of Venus: Implications for atmospheric evolution. Icarus 51, 199–247.

Zhang, X., Liang, M.-C., Montmessin, F., Bertaux, J.-L., Parkinson, C., Yung, Y.L., 2010. Photolysis of sulfuric acid as the source of sulfur oxides in the mesosphere of Venus. Nat. Geosci. doi:10.1038/NGEO989 (published online 31.10.10).